

## Electronic Supplementary Information

# A Bioresponsive Controlled-Release Biosensor Using Au Nanocages Capped with Aptamer-Based Molecular Gate and Its Application in Living Cells

Wei Wang,\* Tao Yan, Shibin Cui, and Jun Wan

State Key Laboratory Base of Eco-chemical Engineering, College of Chemistry and Molecular Engineering, Qingdao University of Science and Technology, Qingdao 266042, P. R. China.

### Materials:

Sodium sulfide nonahydrate ( $\text{Na}_2\text{S}\cdot 9\text{H}_2\text{O}$ ), polyvinylpyrrolidone (PVP, average  $M_r \approx 55,000$ ), Silver Nitrate ( $\text{AgNO}_3$ ), Ethylene glycol, Sodium chloride ( $\text{NaCl}$ ), hydrogen tetrachloroaurate (III) trihydrate ( $\text{HAuCl}_4\cdot 3\text{H}_2\text{O}$ ) and Tris-(2-carboxyethyl)phosphine hydrochloride (TCEP) were purchased from Sigma–Aldrich. Rhodamine B (RhB) was obtained from Shanghai Aladdin Chemistry Corp (China). Adenosine triphosphate (ATP), cytosine triphosphate (CTP), guanosine triphosphate (GTP), and uridine triphosphate (UTP) were obtained from Sigma, and their stock solutions (1.0 mM) were prepared by doubly distilled water. The resulting solution was further consecutively diluted with doubly distilled water in order to obtain the proper solution used for fluorescence detection. The 0.01 M PBS buffer (pH 7.4) was prepared by standard methods. Deionized and doubly distilled water was used throughout the experiments. The synthetic oligonucleotides were purchased from SBS Genetech. Co. Ltd., China. Their sequences are as follows: the ATP-aptamer

sequences, 5' TA TCG ACC TGG GGG AGT ATT GCG GAG GAA GGT GAT CCG GC 3'(S1, red line for the sequences recognized by ATP); the complementary strand, 5'CCA GGT CGA TA TTT TTT-SH-3' (S2); the other complementary strand, 5'-SH-TTT TTT GAT CAC CTT CGA T 3' (S3). The control DNA sequences are as follows: the random DNA sequence, 5' GCC AGC TGG ACC TGG CTA AGG AGC GTG CGA CGG 3'(S4, NOT recognized by ATP); the complementary strand, 5' GGT CCA GCT GGC TTT TTT-SH-3' (S5); the other complementary strand, 5'-SH-TTT TTT CCG TCG CAC GCT 3' (S6). All the chemicals employed were of analytical reagent grade and were used without further purification. Ramos cells were obtained from Chinese Academy of Medical Sciences.

#### **Cell Culture:**

Ramos cells were cultured in RPMI 1640 medium supplemented with 10% fetal bovine serum (FBS) and 100 IU mL<sup>-1</sup> of penicillin-streptomycin. The cells were maintained at 37 °C in a humidified atmosphere (95% air and 5% CO<sub>2</sub>). The amount of cells was determined by using a hemocytometer prior to each experiment. The cells were collected and separated from RPMI cell medium buffer by centrifugation at 3200 rpm for 2 min, followed by washing twice with a sterile phosphate buffer solution (10 mM, pH7.4 PBS). The sediment was resuspended in PBS (1 mL) containing Ca<sup>II</sup> (0.1 mM) and Mg<sup>II</sup> (0.1 mM) to obtain a homogeneous cell suspension (approximately 1.6 × 10<sup>5</sup> cells mL<sup>-1</sup>).

#### **Apparatus:**

30 mm × 60 mm weighing bottles (with caps); a number of magnetic Teflon-coated

stirring bars; temperature-controlled oil bath; Two micropipettes (ranges: 10-100  $\mu\text{L}$  and 100-1,000  $\mu\text{L}$ ) with appropriate disposable tips; Poly(propylene) centrifuge tubes, capacity 50 mL; Poly(propylene) micro-centrifuge tubes, capacity 1.5 mL, 2.0 mL, 5.0 mL and 7.0 mL; 10 mL pipette; spherical condenser; 50-mL round bottom flask with single short neck; Disposable plastic syringe, volume 10 mL with poly (vinyl chloride) (PVC) tubing for solution deliveries; 84-1temperature-controlled magnetic stirring galvanothermy devices (Zhencity Hualu Galvanothermy Instrument Corporation, Shandong, China); TDL-40B centrifuge (Shanghai Anting Scientific Instrument Factory, Shanghai, China); TGL-16B supercentrifuge (Shanghai Anting scientific Instrument Factory, Shanghai, China); glass wares used in the experiment need to be soaked in aqua regia, dried in the oven after cleaning. HHW21-420 electrically heated constant temperature water bath (Tianjin Teste Instrument Corporation, Tianjin, China); Magnetic nanoparticles (MNPs) modified with sulfhydryl groups (3.0~4.0  $\mu\text{m}$ , 10 mg/mL) (SH-MNPs) and a magnetic rack were obtained from BaseLine Chrom Tech Research Centre (Tianjin, China). F-4600 fluorescence spectrophotometer (Hitachi, Japan); THZ-82A constant-temperature air bath oscillator (Jintan Medical Instrument Co. Ltd., Jintan, China); UV-visible spectra were taken with a Cary 50 UV-vis-NIR spectrophotometer (Varian, Agilent). A Nikon E800 inverted microscope with a Nikon Digital sight DS-U1 camera (Nikon, Japan) was employed for fluorescence microscopy imaging. Transmission electron microscopy (TEM) and scanning electron microscopy (SEM) images were taken with JEM-2000EX/ASID2 and JSM-6700F instruments (HITACHI, Japan), respectively.

## Synthesis of Silver Nanocubes

Silver nanocubes were prepared using the sulfide-mediated polyol process as described in the literature with minor modification.<sup>1</sup> Briefly, 6 mL ethylene glycol was placed into a 30 mm × 60 mm weighing bottle which was heated to 150 °C with an oil bath. The solution was kept at this temperature for 1 h under magnetic stirring. Then, 100 µL 3 mM sodium sulfide solution and 1.5 mL 0.18 M polyvinylpyrrolidone solution in ethylene glycol were subsequently added to the bottle. Wait for 10 min. 0.5 mL 0.28 M silver nitrate solution in ethylene glycol was added. Upon injection of the silver ions, the reaction mixture went through a series of color changes that included milky white, light yellow, transparent, red, and ocher. The reaction will be complete in 15 min. Allow the reaction to proceed for 15 min. After that, the reaction was immediately stopped by cooling the bottle in a water bath held at room temperature. The final silver nanocubes was obtained by centrifugation and washed with acetone once and ethanol twice to remove EG and excess PVP and finally re-dispersed in deionized water for further use (4 mL). SEM image (Figure S1, top) and UV-visible absorbance spectra of silver nanocubes (Figure S1, below) are provided here to show the morphology of silver nanocubes and the corresponding UV-visible absorbance peak of the silver nanocubes. The average size of the silver nanocubes was about 50 nm. The UV-visible absorption spectrum of the silver nanocubes showed an absorption peak at 455.3 nm.

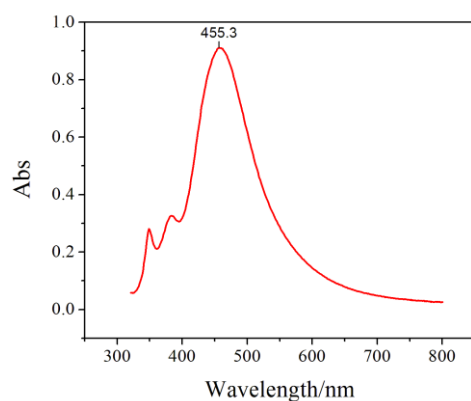
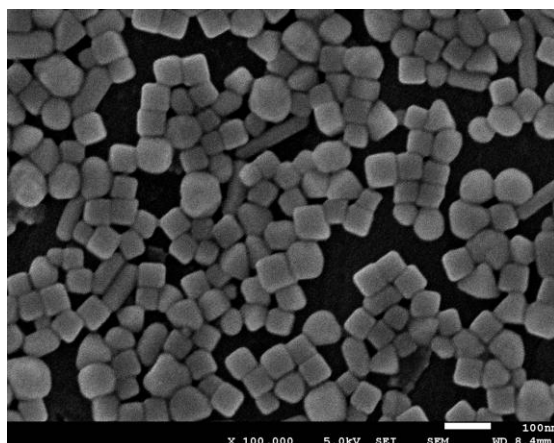


Figure S1. Scanning electron microscope (SEM) image (top) and the UV-visible absorption spectrum of silver nanocubes (below).

## Synthesis of AuNCs

AuNCs were synthesized by means of the galvanic replacement reaction between Ag nanocubes and chloroauric acid ( $\text{HAuCl}_4$ ) with some modification.<sup>2</sup> Briefly, 400  $\mu\text{L}$  of as-prepared silver nanocubes was dispersed in 10 mL water containing 1  $\text{mg mL}^{-1}$  PVP in a 50 mL flask under magnetic stirring. This diluted dispersion of silver nanocubes was then refluxed for 10 min before 6.0 mL of 0.2 mM  $\text{HAuCl}_4$  aqueous solution was added to the flask through a syringe pump at a rate of 0.7 mL solution per minute. The mixture was refluxed for another 10 min until its color became stable.

Once cooled down to room temperature, the sample was centrifuged and washed with saturated NaCl solution to remove AgCl and with water several times to remove PVP and NaCl before characterization by TEM. The edge length of the synthesized AuNCs is  $61 \pm 5$  nm. The UV-visible-near-IR absorption spectrum of Au nanocages (Figure S2) is provided here to show the corresponding Surface Plasmon Resonance peak. According to the literature, the LSPR peaks of AuNCs can be readily and precisely tuned to any wavelength in the NIR region by controlling their size, wall thickness, or both. The spectral results proved that the synthesized AuNCs had a near-infrared LSPR peak at 781.5 nm, indicating that the hollow structure of AuNCs.

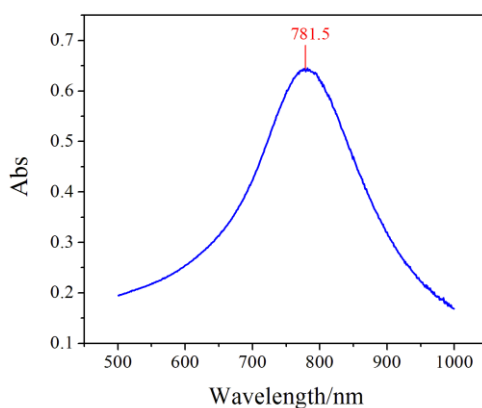


Figure S2. UV-visible-near-IR absorption spectrum of AuNCs.

### **Combination of the AuNCs with MNPs**

Pipette 10  $\mu\text{L}$  MNPs ( $10 \text{ mg mL}^{-1}$ ) into 1.5 mL sample tube, magnetic separation was performed after washing with 200  $\mu\text{L}$  PBS buffer, and the supernatant was discarded with a pipet. This washing procedure is repeated twice. 600  $\mu\text{L}$  of the as-prepared AuNCs suspension was added into the washed MNPs. The mixture was placed in

constant temperature oscillator at room temperature for 10-12 h.

### **Fabrication of the ss-DNAs-AuNCs-MNPs**

Magnetic separate the obtained suspension of the AuNCs-MNPs, and the supernatant was discarded with a pipet. After washing the AuNCs-MNPs thrice with 100  $\mu\text{L}$  PBS, 100  $\mu\text{L}$  of each 1  $\mu\text{M}$  TCEP activated thiol-modified DNAs S2 and S3 were added, respectively, and incubated in constant temperature oscillator at 37  $^{\circ}\text{C}$  for 12 h. The ss-DNAs-AuNCs-MNPs conjugates were “aged” for 24 h by adding 20  $\mu\text{L}$  of 1 M NaCl solution in the system.

### **Loading the nanocages with RhB**

To load fluorescent substance into the hollow interiors of AuNCs, magnetic separation was performed to the obtained ss-DNAs-AuNCs-MNPs suspension, followed by washing the complexes thrice with 100  $\mu\text{L}$  PBS. The washed complexes were resuspended in PBS, 2.4  $\mu\text{L}$  of  $4.8 \times 10^{-4}$  M Rhodamine B solution was added to a final concentration of  $1.2 \times 10^{-5}$  M in a total volume of 100  $\mu\text{L}$ . The complexes were incubated in constant temperature oscillator at 37  $^{\circ}\text{C}$  for 12 h.

### **Fabrication of Aptamer-Based Controlled-Release Biosensor**

In order to cap the holes of the RhB-loaded AuNCs, ATP aptamers were used to hybridize with the two thiol-modified ss-DNAs S2 and S3, which assembled on the surface of the MNPs-combined AuNCs. 100  $\mu\text{L}$  of  $1.0 \times 10^{-6}$  M S1 was added into the above solution. The solution was incubated at room temperature for 2 h. The obtained Apt-RhB-AuNCs-MNPs conjugates were washed three times with PBS buffer solution on a magnetic rack after hybridization procedure. The washed conjugates

were resuspended in 100  $\mu$ L PBS and stored at 4  $^{\circ}$ C for future use. The aptamer-based controlled-release biosensor is completed. Figure S3 shows the fluorescence intensity of GhB released from the hollow interiors of AuNCs. Curve a shows the fluorescence intensity of released RhB without ATP. As indicated in Figure S3, significantly enhanced fluorescence signal was indeed observed in the presence of ATP molecules (curve b).

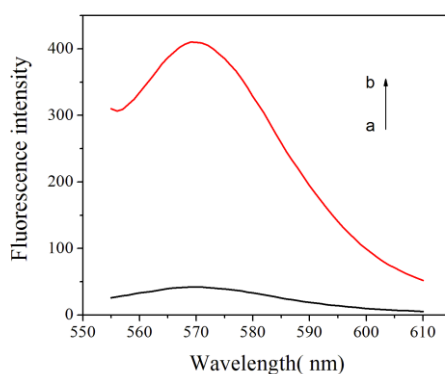


Figure S3. Fluorescence intensity of the solution in the absence (a) and in the presence of  $1.0 \times 10^{-5}$  M of ATP (b).

### ***In vitro* Probing Based on the Controlled-Release Apt-AuNCs Systems**

To test the ability of *in vitro* probing of the Apt-AuNCs system, we carried out the detection of ATP by employing the fabricated controlled-release Apt-AuNCs-MNPs complex based on the proposed platform. The release of RhB was triggered by addition of ATP molecules to the Apt-AuNCs-MNPs system. In the presence of target molecules, the double helixes were opened through a competitive displacement

reaction, and the aptamer would be uncapped from the AuNCs system. Therefore, it was expected that the release of RhB would be sensitive to the ATP molecule. The mixture of APT molecules and Apt-AuNCs-MNPs were subjected to incubation at 37 °C for 30 min to ensure the full reaction between the aptamer and ATP. After magnetic separation, the supernatant was kept for fluorescence detection with an excitation wavelength at 530 nm and an emission wavelength at 573 nm. Figure S4 shows fluorescence intensity of GhB released from the hollow interiors of AuNCs after injection of ATP with different concentrations. These results demonstrate that aptamer can play the role of molecular gate effectively, and the fabricated bioresponsive controlled-release Apt-AuNCs-MNPs system is an efficient biosensor for target molecules detection through aptamer-target binding. Fluorescence signals of GhB released from the hollow interiors of AuNCs with increasing levels of ATP (a) 0, (b)  $1.0 \times 10^{-7}$  M, (c)  $2.0 \times 10^{-7}$  M, (d)  $4.0 \times 10^{-7}$  M, (e)  $1.0 \times 10^{-6}$  M, (f)  $2.0 \times 10^{-6}$  M, (g)  $1.0 \times 10^{-5}$  M.

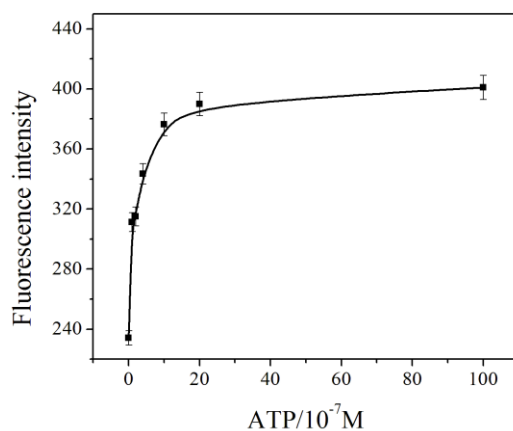


Figure S4. Controlled release of GhB released from the hollow interiors of AuNCs triggered by

ATP as a function of concentration.

### **Determination of ATP in a Cultured Cell Extract**

To test the validation of the platform for real-world samples, analysis of cellular ATP from Ramos cell extracts was implemented. A suspension of  $1.6 \times 10^5$  Ramos cells (1.0 mL) dispersed in RPMI cell media buffer was centrifuged at 3000 rpm for 5 min and washed with phosphate-buffered saline (18.6 mM phosphate, 4.2 mM KCl, and 154.0 mM NaCl, pH7.4) five times and resuspended in 200  $\mu$ L of deionized water. Finally, the cells were disrupted by sonication for 20 min at 0 °C. To remove the homogenate of cell debris, the lysate was centrifuged at 18 000 rpm for 20 min at 4 °C. After adding the cell lysate into the Apt-AuNCs-MNPs, the mixtures were subjected to incubation at 37°C for 30 min to ensure the full reaction between the aptamer and ATP. After magnetic separation, the supernatant was kept for detection. The fluorescence signal was significantly enhanced as compared with blank control. The concentration of ATP in the Ramos cell lysate is  $8.0 \times 10^{-7}$  M per  $1.6 \times 10^5$  cells.

### **Fluorescence microscopy imaging of Ramos cells**

The fluorescence microscopy imaging was performed by incubating Ramos cells with the Apt-AuNCs system in growth media for 1 h at 37°C. Au nanocage modified with random DNA that can bind with SH-DNA while inert to ATP was used as a control under the same conditions. A Nikon E800 inverted microscope fitted with a Nikon

Digital sight DS-U1 camera was employed for fluorescence microscopy imaging.

## Optimization of incubation temperature for the ATP-aptamer binding

To get the optimal incubation temperature for the ATP-aptamer binding, measurements were conducted at 37 °C and 25 °C, respectively. The incubation time was 0.5 h. The concentration of the cap oligonucleotides was  $1 \times 10^{-6}$  M and ATP was  $5 \times 10^{-6}$  M. Figure S5 shows the fluorescence intensity after incubated for 0.5 h at 25 °C and 37 °C, respectively. The results indicate that the enhanced fluorescence intensity ( $\Delta F$ ) at 37 °C was obvious bigger than that at 25 °C. As a result, 37 °C was taken as the optimal incubation temperature for the ATP-aptamer binding.

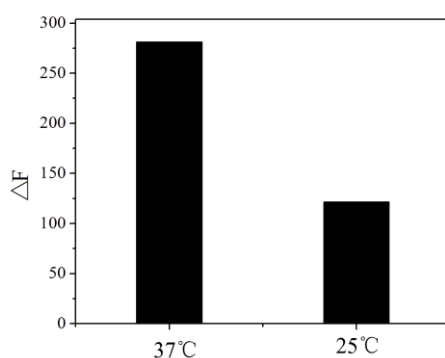


Figure S5. The fluorescence intensity after incubated for 0.5 h at 25 °C and 37 °C, respectively.

$\Delta F$  is fluorescence intensity after blank deduction.

## Optimization of incubation time for the ATP-aptamer binding

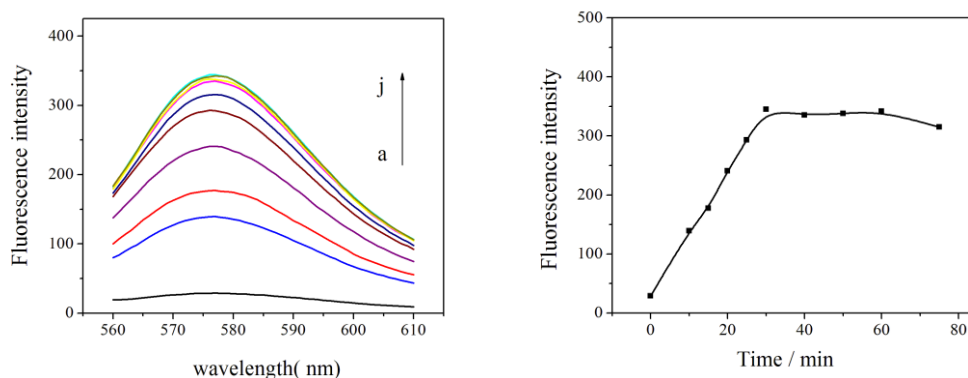


Figure S6. The fluorescence intensity changes with time.

Reaction time is also an important factor and the incubation time for ATP-aptamer binding was investigated. The concentration of the cap oligonucleotides was  $1.0 \times 10^{-5}$  M and ATP was  $5.0 \times 10^{-6}$  M. As shown in Figure S6, when the reaction time ranges from 0 min to 75 min while keeping the incubation temperature constant at 37 °C, the fluorescence intensity is enhanced with the increase of time and then levels off at time 30 min. That is to say, 30 min was essential for the accomplishment of ATP-aptamer binding.

## References

- [1] Skrabalak, S. E., Au, L., Li, X.; Xia, Y. Facile synthesis of Ag nanocubes and Au nanocages. *Nature Protocols* **2007**, 2, 2182.
- [2] Sun, Y.; Xia, Y. Shape-controlled synthesis of gold and silver nanoparticles. *Science* **2002**, 298, 2176.